Al-Mukhtar Journal of Engineering Research 07 (1): 29-42, 2023
Doi:

Research Article **Open Access**

Vibration damping using granular materials

Saleh S. H. Emtaubel [(1)], Galal Hamed Senussi [(2)], Jim A. Rongong [(3)]

***Corresponding author:** saleh.emtobel@omu.edu.ly
Faculty of Mechanical Engineering, Omar Al Mukhtar university, Libya.

Second Author: , galal.senussi@omu.edu.ly
Faculty of Mechanical Engineering, Omar Al Mukhtar university, Libya

Third Author: j.a.rongong@sheffield.ac.uk,
Faculty of Mechanical Engineering, University of Sheffield, UK

Received:
17 July 2023

Accepted:
30 November 2023

Publish online:
31 December 2023

Abstract

The aim of this paper is to study experimentally and numerically the effects of vibration amplitude and frequency on the performance of granular systems, with a view to optimizing their use in reducing vibrations typically experienced in machinery. Granular material systems are highly nonlinear systems and, as such, have multiple factors that will affect any experiment. This nature of granular material systems caused some discrepancies between experiment results and the simulations of mathematical models. However, the nonlinear aspect of particle damping restricted researching its theory, but the experiment research has largely surmounted that limitation. Experimental results suggested several damping theories. Accordingly, the ability to reduce vibrations of particle dampers depends on several external and internal factors. The two external factors are excitation amplitude and its frequency, whereas the internal factors are related to the properties of the particles and the size of the container. Other internal factors relate to the mass ratio of total particles to the primary structure and particle placement. The experimental work included developing a computational single degree of freedom (SDOF) model to provide better understanding of the effect of shock vibration and work with the future experimental work.

Keywords: Damper, Vibration, Excitation, Frequency, beam.

INTRODUCTION

Particle dampers are devices that control vibration levels in structures. They function by an impact and friction damping together. The primary structure's energy is transferred to the particles inside the damper's casing that is attached to the vibrating system where it dissipated by being absorbed by the action of the contacts between the particles. The principal processes engaged in energy dissipating are: collisions, sliding friction and rolling friction with those processes taking place between the particles and with the particles and the damper casing's walls. This type of damping can be optimized by adjusting the acceleration of the particles within the container [1]. At lower frequencies, the damping mechanism requires that the particles and the casing wall to be out-of-phase with one another resulting in comparatively empty container. Particle impact dampers originated from impact dampers and they are more efficient in reducing vibrations than them [2]. Another key mechanism operating inside particle dampers is associated with the granular material's state of matter. For example, at high amplitude frequencies gas-like states occur whereas at lower frequencies solid and liquid-like states appear. In this damping mechanism, performance can be optimized by paying attention to the state of the particles in the container [3].

Particle dampers are used in several industries to limit vibrations and noises. The aerospace industry led the way in using them, however; other industries such as automotive, medical and energy soon followed [4]. There are many particle dampers' applications in strengthening buildings against earthquake and in automotive gears to suppress vibrations in the rotary shaft of gear transmission. There are other uses in helicopter and aircraft mechanisms in rotor blades and landing gears, and in machine tools. Noise resulting from machine actions can also be reduced by impact dampers [5], however; at times the actions of the impact dampers can increase it [2].

The use of granular materials to reduce resonant vibrations in machinery and structures is increasing. They are attractive because they combine several different energy dissipation mechanisms, making them more versatile than traditional damping materials. This study sets out to understand and model the effects of vibration amplitude and frequency on the performance of granular systems, with a view to explaining and optimizing their use in reducing vibrations typically experienced in machinery.

Numerical modelling will be used alongside laboratory experiments to investigate the effects on energy dissipation performance of features such as particle material, shape, and the geometry of a flexible–walled packet container. The experiments described in this study were devised to give some introductory understanding of single particle damping. They were also intended to identify key variables and to direct the design of future experiments. The experiment was to investigate the damping performance of a single particle (viscoelastic sphere) placed within a cavity attached to a vibrating beam. First, the resonance of the beam plus empty damper was considered and then the natural frequency and modal damping ratio for different amplitudes and damper gap settings are identified.

Finally, the SDOF mathematical model is used to write a MATLAB code for a simulation to estimates time domain response for a SDOF impact damper using measured parameters obtained and the numerical results are then compared with the single particle impact damper experimental results.

MATERIALS AND METHODS

This experiment Investigated the resonance of a beam with a single damper attached and identified the first natural frequency and modal damping ratio for different amplitudes. The experimental analysis is performed with the system shown in figure 1.

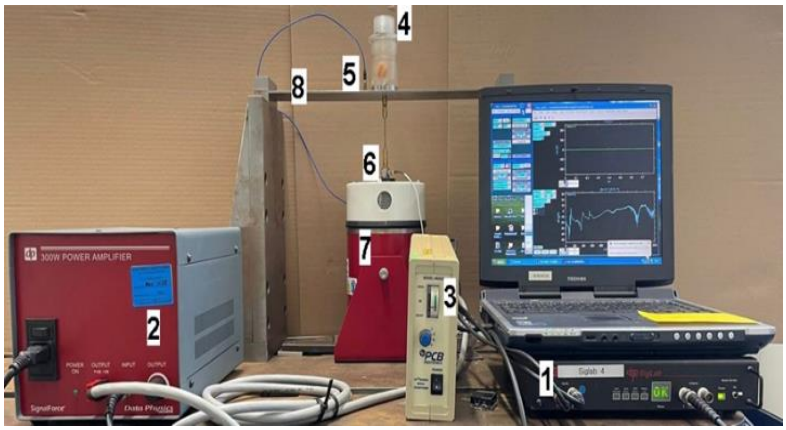

Fig. 1 Impact damper experiment setup

Table (1): Description of individual components

	SigLab 4 signal analyser
	300W power amplifier
	PCB model 482A22 charge amplifier
	Particle damping enclosure (empty)
	PCB 353B18 accelerometer (Sensitivity 981 m/s^2/V)
	PCB 208B01 force transducer (Sensitivity 8.99 N/V)
	Electromagnetic shaker (peak sine force capacity 100 N)
	Clamped steel beam 425L x 75W x 4D (mm)

The test structure is a steel beam that is clamped at either end. The beam has a cross-section that is approximately 75x4 mm and the free length between the clamps is approximately 425 mm. A casing of the damper (of mass 266.6 grams) is attached to the beam using a threaded connector.

The system is excited by an electrodynamic shaker via a stinger rod. The force applied by the exciter is measured with a force transducer and the beam vibration is measured with an accelerometer. Signals from these transducers are recorded on a data acquisition system (Table 1, Fig. 2). The test rig is adjusted such that the direction of shaking aligns with the direction of gravity. The vibration response is measured over a frequency range of around 10-1000 Hz using signals of varying magnitude and frequency content. The amplitude will be in the range 1 to 1000 m/s^2.

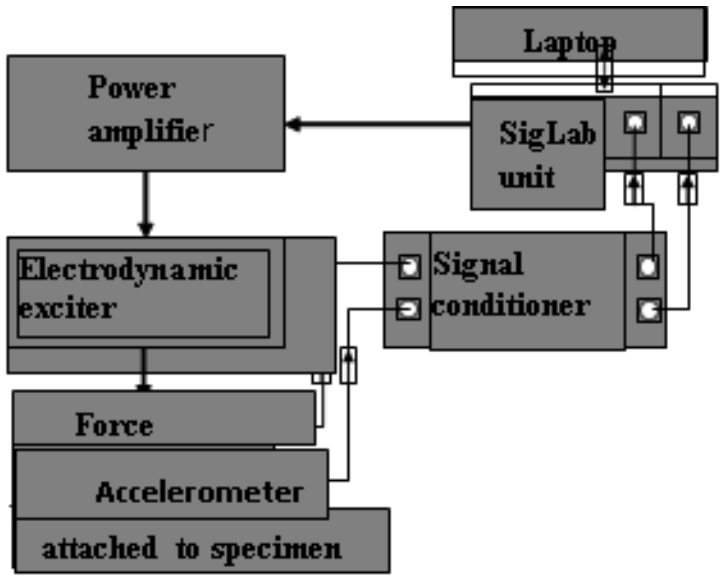

Fig. (2) Signal flow diagram

The impact damper's container as shown in Fig. 3 is similar to the damper used by Wong et al. [6]. It is constructed from a clear PMMA cylinder so the movement of the sphere can be noticed with a steel base. The container has a threaded top for gap size adjustment. A viscoelastic sphere(rubber) of mass 11.5 grams and diameter ≈ 25mm is placed in the container.

Natural frequency (ω_n) and damping ratio (ζ) measurements of the system were taken at gap sizes of 0 (lid firmly on top of sphere), 10, 15, 23 millimeters; and for random excitation 19 values of acceleration with an increment of 0.1g at accelerations of 0.07 to 1.7 g and for sin-ewave excitation 19 values of excitation acceleration with an increment of 0.1g from 0.05 to 5.0

g.

For random excitation, the SigLab virtual network analyzer (vna) was used which provides links to network-based analysis tools for measuring frequency response functions. Information was retrieved from (vna) data file, then the post process was done in the MATLAB setting using the SLm data structure using the MATLAB function frf_from_vna in

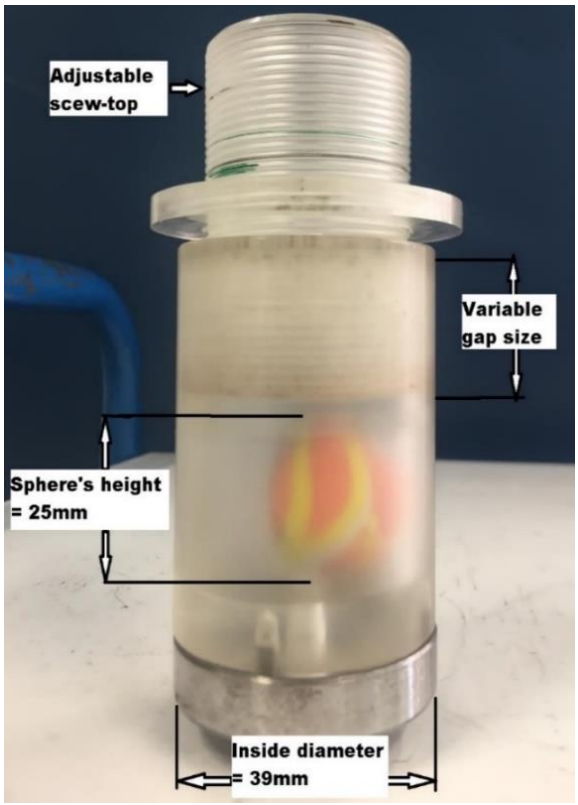

Fig (3). Damper container with adjustable gap

combination with the function from_frf to get the natural frequency and damping ratio from frf uses functions mobfit and mobfit_obj to curve fit. For sinewave excitation from the SigLab swept-sine analyzer (vss) was used for measuring the system's frequency response function. The data processing was done sing the MATLAB function frf_from_vss.

As for the repeatability and uncertainty in the results, there is a major problem connected with random excitation is that signals will always experience leakage. This leakage error will cause a serious reduction of the quality of the measured frequency response function (frf), with a sizable error resulting, mainly at the resonant peaks of the system **[7]**. Leakage is also an issue for sinewave excitation.

RESULTS AND DISCUSSION

Vibrating beam's natural frequency and modal damping ratio

First, the resonance of a vibrating beam is investigated and the natural frequency and modal damping ratio (ζ) for different amplitudes are identified. There is a difference in the damping ratio (ζ) trend between the different excitations as the damping ratio for random excitation is almost constant with the increasing amplitude whereas the damping ratio for sinewave excitation increases with the increasing amplitude (Fig. 4).

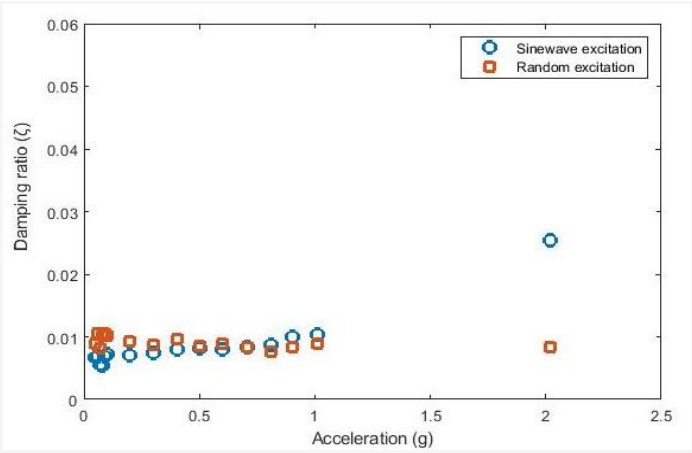

Fig. (4). The acceleration's (g) effect of on the damping ratio (ζ) for random and sinewave excitations

The results of the natural frequency (ω_n) for the different excitations are illustrated in fig. 5, where the beam response to random and sinewave excitation show the same trend.

If there is a resistance to the vibrations when the system is undamped then the system undergoes frictional or other type of loss of kinetic energy which is damped with time. The energy loss within the structure itself is called structural (hysteresis) damping where in solids some of the energy involved is the repetitive internal deformation and restoration to the original shape is dissipated in the form of random vibrations of an intramolecular nature. Most likely this is friction damping at the joints since metals have a loss factor of less than 0.001 and the PMMA damper does not significantly deform in the 10-100 Hz range.

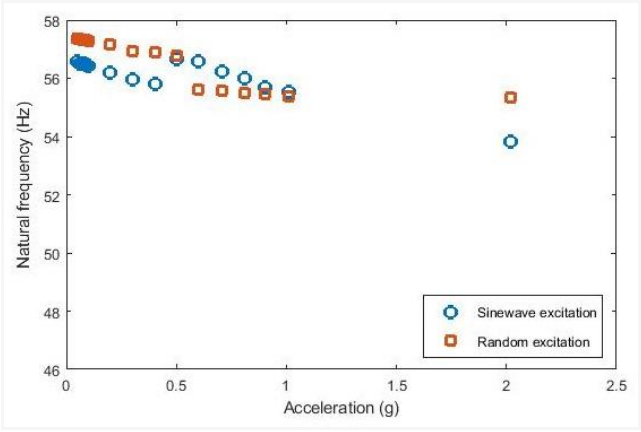

Fig. (5) Comparison of the acceleration's (g) effect of on natural frequency (ω_n) for random and sinewave excitations of a steel beam

The effects of gap size of an impact damper under random and sinewave excitation

When a continuous structure vibrates with a particular deflection shape, its motion can be represented by a SDOF system. The mass of this equivalent system is obtained using the equivalent kinetic energy. For slender uniform beams, the equations for normal vibration mode shapes are given in textbooks [8]. For these, they also show that for equal kinetic energy in both systems,

$$\frac{1}{2}\dot{y}_{SDOF}^2 m_{eq} = \frac{1}{2}\dot{q}^2 m \quad \Rightarrow \frac{1}{2}\dot{y}_{SDOF}^2 m_{eq} = \frac{1}{2}\left(\frac{y_{SDOF}}{\phi_i}\right)^2 m$$

where φ defines the shape of the deflection as a function of the distance along the beam and therefore,

$$m_{eq} = \frac{m}{\phi_i^2}$$

At the end of a cantilever the fundamental vibration mode shape gives $\varphi^2 = 4$, at the mid-point of a clamped-clamped beam $\varphi^2 = 2.52$ and at the mid-point for a pinned-pinned beam $\varphi^2 = 1$.

The beam has a cross-section that is approximately 75x4 mm and the free length between the clamps is approximately 425 mm.

The test structure is a steel beam that is clamped V= (L) (H) (W)

V = (0.425) (0.075) (0.004)

$= 1.275 \times 10^{-4}\ m^3$

ρ (For steel) = 7900 kg/m^3

The mass, m = (v) (ρ)

$= (1.275 \times 10^{-4}\ m^3)\ (7900\ kg/m^3)$

$= 1.00725$ kg

At the mid-point of a clamped-clamped beam $\varphi^2 = 2.52$

$$m_{eq} = \frac{m}{\phi_i^2}$$

$$= \frac{1.00725}{2.52}$$

$$= 399.7\ g$$

The mass of sphere = 11.5 g

The mass of empty container = 266.6 g

So, The Total mass is:

$m_t = 11.5 + 266.6 + 399.7$

$= 677.8$ g

First there is a discussion of random excitation results followed by the sinewave results. When the system is subjected to random excitation and for a gap size of 0 mm, even though the sphere does not have any space to move and this does not allow for significant interchange of momentum between the sphere and the container, the nature of random excitation high frequency causes the particle to have more movement. Therefore, it has dissipation of energy and the measured damping ratio is higher than 23 mm and 10 mm gaps (Fig. 6). As the gap size increases, the particles are given more room to move and the damping ratio (ζ) reaches 0.04104 at acceleration amplitude 1.7g which occurs at an optimum gap size of 15 mm. If the gap size is increased further there will be fewer impacts since the particle does not acquire enough velocity to travel from bottom of the container to the top, on the average twice per "cycle" of the response. Therefore, if the gap size is increased beyond the optimum, the damping decreases.

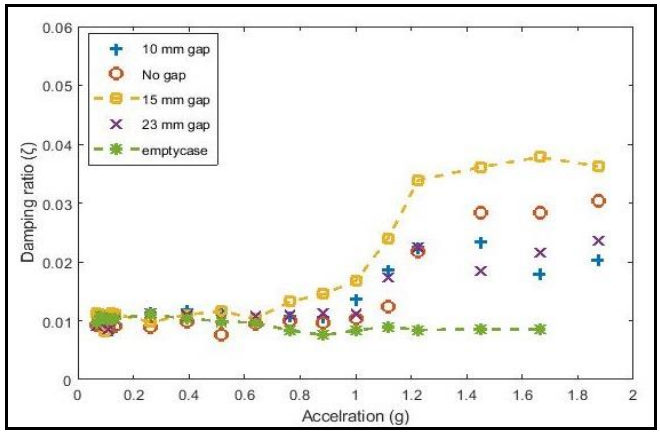

Fig. (6). The effect of acceleration g (rms) on the different gaps of an impact damper's damping ratio (ζ) under random wave excitation

The damping ratio at optimum gap size increases with increasing acceleration. Overall, the damping ratio of the beam was increased by over five times, demonstrating the effectiveness of the particle impact damper particularly at high amplitudes of excitation (Fig. 7). Experiments also revealed a shift in the resonance frequency of the system. This frequency shift is affected by both acceleration and gap size. Figure 8 shows that the resonance frequency decreases with increasing acceleration

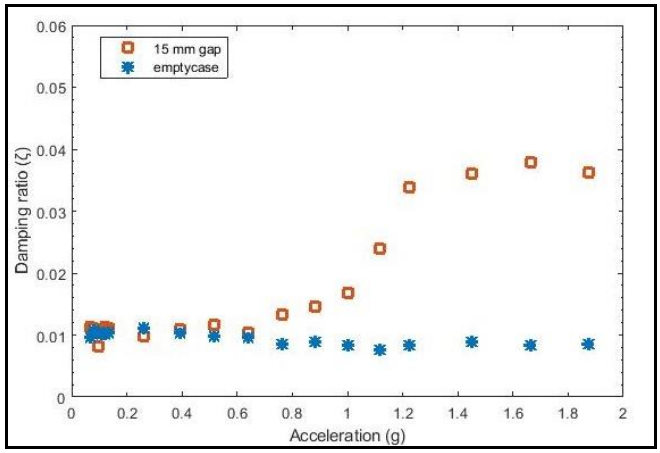

Fig. (7) Comparison of the acceleration g (rms) effect on the damping ratio (ζ) of an impact damper (with 15mm gap) to that of an empty-case under random wave excitation

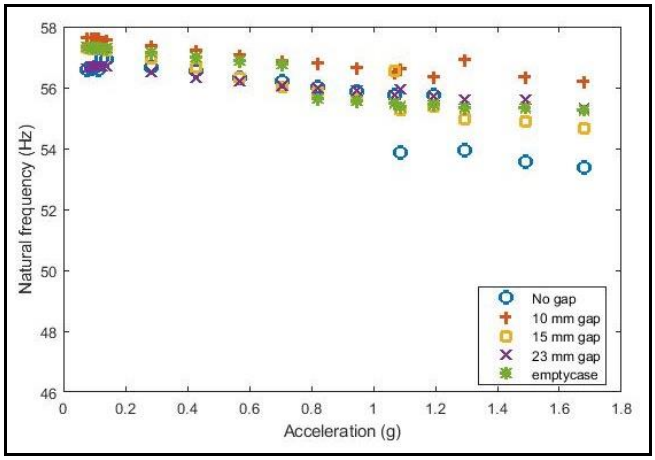

Fig. (8) The effect of acceleration g (rms) on the different gaps of an impact damper's natural frequency (ω_n) under random wave excitation

for all gap sizes at different rates. This confirms that as the sphere has more space to move, it contacts the container less resulting in a lower mass effect and higher resonance frequency. With the increase of acceleration, a higher mass effect is produced, which implies that the sphere has more contacts with the container. Overall, the natural frequency of 15 mm gap under random excitation is lower than that of the beam's natural frequency.

The damping ratio (ζ) values of the system under sinewave excitation exhibits show almost the same trend with the different gaps as the random excitation with the exception that the effective damper's gap is 10 mm which is smaller than that determined by random excitation (Fig. 9). The damping ratio of this gap is more than three times higher than that of the empty-case's damping (Fig. 10).

The natural frequency (ω_n) of the system under sinewave excitation exhibits a different trend than that of

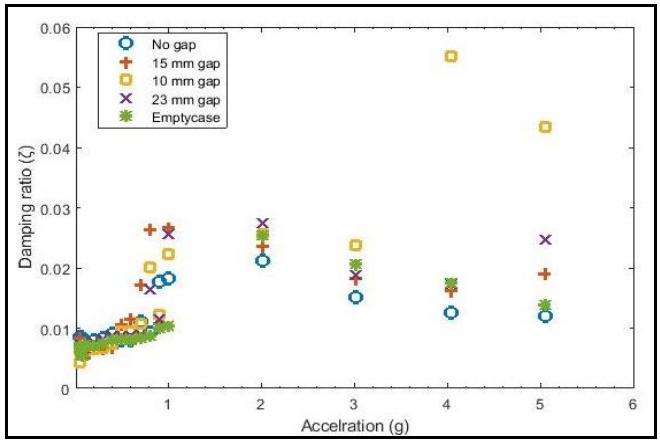

Fig. (9) The effect of acceleration g (peak) on the different gaps of an impact damper's damping ratio (ζ) under sinewave excitation

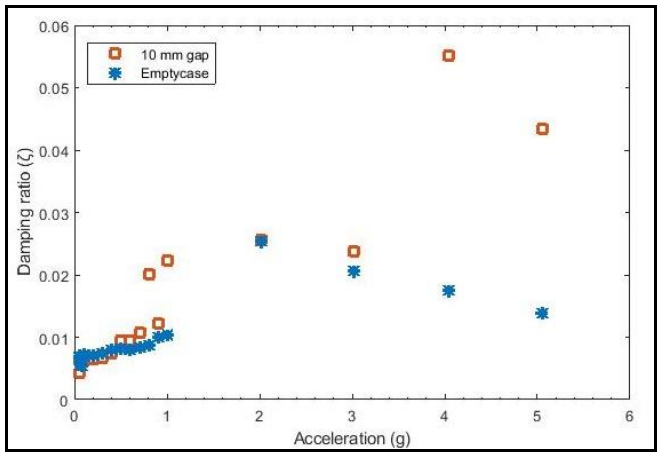

Fig. (10) Comparison of the acceleration g (peak) effect on the damping ratio (ζ) of an impact damper (with 10mm gap) to that of an empty-case under sinewave excitation

the random excitation in that the natural frequency of the 10mm gap is lower than the damper with no gap (Fig. 11). And it is much lower than the empty-case's natural frequency as shown in figure 3.11.

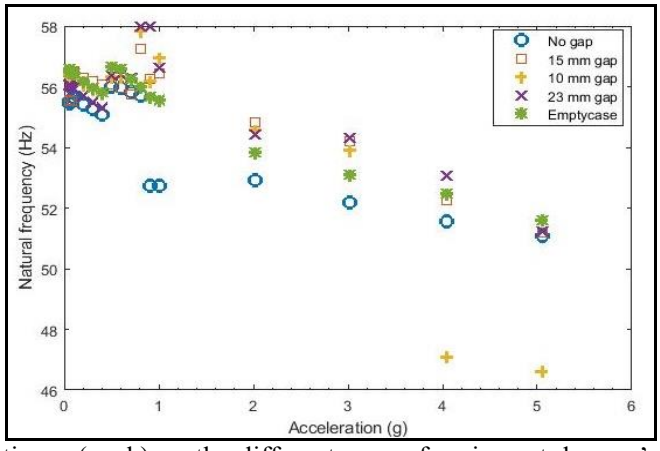

Fig. (11) The effect of acceleration g (peak) on the different gaps of an impact damper's natural frequency (ω_n) under sinewave excitation

DISSIPATED ENERGY IN THE SYSTEM

If a vibrating system is connected to a damper, then due to damping, the amplitude will reduce in each cycle. This is because it is the rule of damping to reduce the amplitude and since the amplitude is reduced in each cycle, it means that energy of the system is dissipated. Thus, the damping in this system is reducing the amplitude by absorbing some energy of the vibrating system, so the dissipated energy of the system under sinewave excitation with gap 10 mm and amplitude 5g is determined by the equation (Appendix C):

$$W = \pi\, c\, \omega\, X^2$$

Stiffness and damping for impact damper:

$$\omega_n = 2\pi f$$

$$= 2\ (3.1415)\ (46.62)$$

$$= 292.91\ rad/s$$

Accounting for the background damping of the test rig:

$$\zeta_{(actual)} = \zeta_{measured} - \zeta_{\ test\ rig}$$

$$= 0.04333 - 0.01382 = 0.02951$$

$$c = 2\zeta m \omega_n$$

$$= 2\ (0.02951)\ (0.6778)\ (292.91)$$

$$= 11.72\ Ns/m$$

Calculating the amplitude's value, $A = X\omega_n^2$

$$X = \frac{A}{\omega_n^2}$$

$$= 49.05 / (292.91)^2$$

$$= 5.7 \times 10^{-4}\ m$$

Dissipated energy (W):

$$W = \pi\, c\, \omega\, X^2$$

$$= (3.1415)\ (11.72)\ (292.91)\ (5.7 \times 10^{-4})^2$$

$$= 3.5 \times 10^{-3}\ J$$

Kinetic energy (T):

$$T = {}^1/_2\ m_p\ (\omega X)^2$$

$$= ½\ (11.5)\ [(292.91)\ (5.7 \times 10^{-4})]^2$$

$$= 1.6 \times 10^{-4}\ J$$

Calculation of W/T ratio from impact damper:

The Specific damping capacity (ψ) = W/T is calculated from excitation amplitude 0.1 to 5 g as in Table 2.

Table 2: Ratio of dissipated energy per cycle (W) to kinetic energy per cycle (T)

Amplitude (X) m	Kinetic energy per cycle (T) J	Dissipated energy per cycle (W) J	W/T
7.9×10^{-5}	4.5×10^{-8}	3.1e-8	0.7
1.6×10^{-5}	1.8×10^{-7}	7.0e-8	0.4
2.4×10^{-5}	4.1×10^{-7}	2.4e-7	0.6
1.3×10^{-5}	1.2×10^{-7}	5.8e-8	0.5
3.3×10^{-5}	7.8×10^{-7}	7.9e-7	1.0
4.7×10^{-5}	1.5×10^{-6}	1.8e-6	1.2
5.5×10^{-5}	2.2×10^{-6}	3.6e-6	1.6
6.0×10^{-5}	2.7×10^{-6}	2.3e-5	8.5
7.1×10^{-5}	3.6×10^{-6}	5.9e-6	1.6
7.7×10^{-5}	4.4×10^{-6}	3.8e-5	8.6
1.7×10^{-4}	2.0×10^{-5}	4.7e-6	0.2
$2.6\ \chi\ 10^{-4}$	4.5×10^{-5}	1.0e-4	2.2
4.5×10^{-4}	1.0×10^{-4}	2.8e-3	28
5.7×10^{-4}	1.6×10^{-4}	3.5e-3	6.1

One of the simplest ways to model a single particle impact damper is to use a SDOF model in which the particle is represented by mass that can move between rigid walls, which themselves are subject to prescribed motion. The contact between the particle and the walls of the casing can be represented by springs and dampers as shown in figure 12.

The variables x_c and x_p represent the positions of one of the walls and the particle relative to an arbitrary fixed point in space. The second wall remains a fixed distance L from the first one. When the casing walls move with a prescribed time history, useful outputs of the model are the resulting motion of the particle and the force required to maintain the motion of the casing.

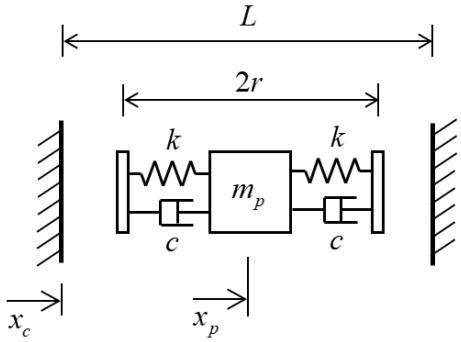

Fig. (12). An SDOF model showing contact between the particle and the casing

Motion of the particle is related to force applied to it using Newton's Second Law,

$$m_p \ddot{x}_p = f$$

It can be seen from the figure that particle-wall contact is not constant and hence the force depends on the contact conditions. No force is transmitted when the particle is not touching a wall. In the absence of body forces such as gravity loading, $f = 0$.

When in contact, force is generated by spring and damper units. However, even when in contact, the spring and damper together cannot exert a tensile force. These conditions are summarised in Table 3.

Time domain simulation

The equation of motion can be solved numerically in Matlab using the function ode45. This function provides a numerical solution to a first order differential equation of the form,

$$\dot{\boldsymbol{y}} = \boldsymbol{A}\boldsymbol{y} + \boldsymbol{F},$$

For the impact damper problem this can be achieved by setting

$$\boldsymbol{y} = \begin{bmatrix} x_p \\ \dot{x}_p \end{bmatrix} \quad \text{and,} \quad \boldsymbol{A} = \begin{bmatrix} 0 & 1 \\ -\frac{k}{m_p} & -\frac{c}{m_p} \end{bmatrix}$$

Table (3): Conditions of particle contacts

	Contact with the cylinder bottom	**Contact with the cylinder top**
Condition	$\boldsymbol{x_c \geq x_p - r}$	$\boldsymbol{x_c \leq x_p + r - L}$
Force *f*	$f = f_{spring} + f_{damper}$ $f_{spring} = -k\left(x_p - r - x_c\right)$ $f_{damper} = -c\left(\dot{x}_p - \dot{x}_c\right)$	$f = f_{spring} + f_{damper}$ $f_{spring} = -k\left(x_p + r - x_c - L\right)$ $f_{damper} = -c\left(\dot{x}_p - \dot{x}_c\right)$
No tension	$\boldsymbol{f > 0}$	$\boldsymbol{f < 0}$

In this example, excitation is in the form of prescribed harmonic motion of the casing and the forcing vector depends on the contact,

Contact with the cylinder bottom:

$$\boldsymbol{F} = \begin{bmatrix} 0 \\ \frac{k}{m_p}(x_c + r) + \frac{c}{m_p}\dot{x}_c \end{bmatrix}$$

Contact with the cylinder top:

$$\boldsymbol{F} = \begin{bmatrix} 0 \\ \frac{k}{m_p}(x_c + L - r) + \frac{c}{m_p}\dot{x}_c \end{bmatrix}$$

If the motion of the casing is sinusoidal,

$$x_c = X_c\, sin(\omega t)$$
$$\dot{x}_c = \omega X_c\, cos(\omega t)$$

The Matlab expression for running the time domain solution has the following form,

[t,y] = ode45('calc',t,y_0);

where t is an array containing the discrete points in time that the solution y is obtained at and y_0 are the starting values. The term 'calc' refers to a function "calc.m" that specifies the differential equation and provides the output $\dot{y}$ (written y_d) for a given input (y) at a particular time (t).

y_d = calc(t,y)

For this particular example, it is convenient to note that,

$$\dot{\boldsymbol{y}}(1) = \dot{x}_p = \boldsymbol{y}(2)$$

and,

$$\dot{\boldsymbol{y}}(2) = \ddot{x}_p = \frac{f}{m_p}$$

where the force *f* depends on the contact conditions defined on the previous page.

This entire example has been coded into the function sdof_impact_damper. Because of the limitation on allowed input and output variables in "calc.m" this function has to encode internal computations to allow the force to be specified. To allow convenient adjustment of the values of variables, the main function sdof_impact_damper rewrites "calc.m" each time it is run.

simulation and comparison to experimental results

In this section, the mathematical model is verified and used to perform the simulation with damping and stiffness parameters obtained from the drop-bounce experiment and system parameters with the vibration amplitude (defined as beam displacement X_c) matching the peak vibration in the experimental tests (Table 4, Fig. 13).

Table (4): Parameters used in the simulation

Particle and system parameters	
Particle mass m	11.5 x 10^{-3} m
Particle radius	12.5 x 10^{-3} m
Stiffness k	40.76 x 10^{3} N/m
Damping c	0.7 Ns/m
Casing length L	40 x 10^{-3} m
Excitation frequency whz	46.62 Hz
Amplitude Xc	5.7 x 10^{-4} m

The specific damping capacity (ψ) W/T per cycle of the simulation is calculated and compared to that of the impact damper experiment (Table 5). There is a small discrepancy between the simulation and experimental results (Fig. 14).

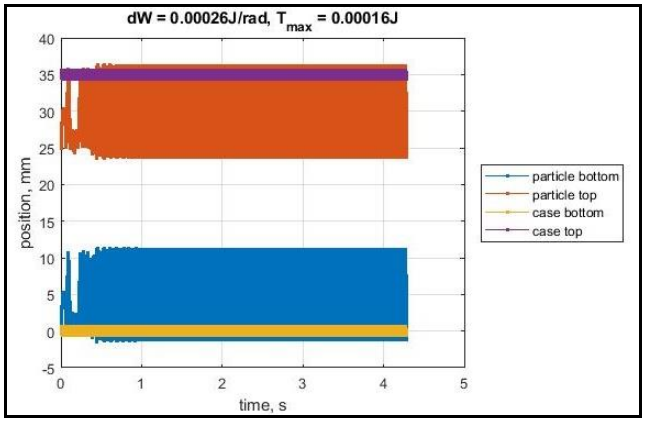

Fig. (13). simulation showing the dissipated energy by radian resulting from a viscoelastic sphere contact with the damper's casing at vibration amplitude (Xc) 5.7 x 10^{-4} m and excitation frequency 46.62 Hz

CONCLUSION

The practical and inert vibration control technology of particle damping is developing considerably at the present stage with ongoing research into its many factors. This study aims to explore the role of contact pressure of the particles and the configuration of its container.

Table 5: Comparing the specific damping capacity (W/T) of experiment and simulation

Amplitude (X) m	W/T simulation	W/T experiment
7.9 X 10^{-6}	0	0.3
4.7 X 10^{-6}	0	1.9
5.5 X 10^{-6}	0	0.5
6.3 X 10^{-6}	0	0.5
7.0 X 10^{-6}	0	0.5
7.9 X 10^{-6}	0	0.7
1.6 X 10^{-5}	0	0.4
2.4 X 10^{-5}	0	0.6
1.3 X 10^{-5}	0	0.5
3.3 X 10^{-5}	0	1
4.7 X 10^{-5}	0.7	1.2
5.5 X 10^{-5}	1.9	1.6
7.1 X 10^{-5}	1.2	1.6
1.7 X 10^{-4}	1.2	0.2
2.6 X 10^{-4}	3.8	2.2

The identification of the main challenge: granular damper properties strongly affected by the extent to which

particles are forced together to form temporary agglomerations such as what is seen in the "bouncing bed" phase. The ability to form and adjust the nature of these agglomerations gives control over the damper effectiveness, so this research focuses on physical ways of controlling this.

The discrepancy between the simulation and experimental results could be caused by the level of uncertainty in the damping ratio data which is showing in the quality of the circle-fit which artificially effect the damping. This uncertainty could be also caused by the nonlinearity

of the system or could be an issue with the shaker drop-out causing more vibrations. Thus, measurements of natural frequency data have a higher level of certainty than the damping ratio data. Considering the uncertainty in the experiment the comparison result is a reasonable outcome.

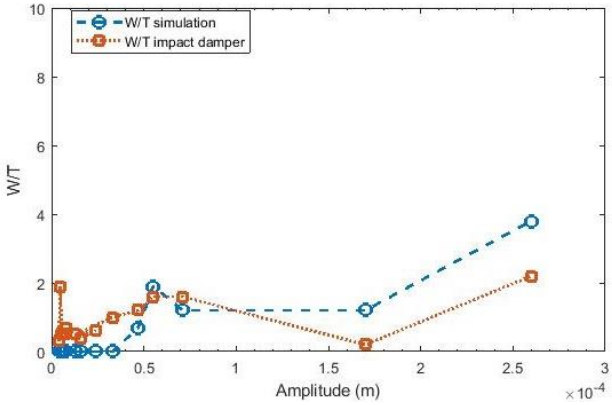

Fig. (14). Comparing the specific damping capacity (W/T) of experiment and simulation

The flexible packet is one way to adjust the agglomerations in a controllable manner. Thus, future work

will concentrate on the design and experiment of a flexible packet damper that can be used to adjust the particle-to- particle contact pressure (and therefore the performance) of a granular damper. The flexible packet comprises a collection of particles that are squeezed together by an elastic membrane which provides a nominal static pressure that is defined by the tension in the membrane. The membrane can be constructed from different materials, but initial work will involve an elastomer for simplicity.

REFERENCES

[1] S. Masri and A. Ibrahim, "Response of the impact damper to stationary random excitation," *J. Acoust. Soc. Am.*, vol. 53, no. 1, pp. 200-211, 1973.

[2] R. Ibrahim, Vibro-Impact Dynamics, Modelling, Mapping and Applications, Berlin: Springer-Verlag Berlin Heidelberg , 2009.

[3] C. Saluena, T. Pschel and S. Esipov, "Dissipative properties of vibrated granular materials," *Phys. Rev. E,* vol. 59, no. 4, pp. 4422-44, 1999.

[4] M. Sanchez, C. Carlevaro and L. Pugnaloni, "Effect of particle shape and fragmentation on the response of particle dampers," *J. Vib. Control ,* vol. 20, no. 12, pp. 1846-1854, 2014.

[5] A. Oldzki, I. Siwicki and J. Winiewski, " Impact dampers in application for tube, rod and rope structures," *Mech. Mach. Theory ,* vol. 34, no. 2, pp. 243-253, 1999.

[6] C. Wong, M. Daniel and J. Rongong, "Energy dissipation prediction of particle dampers," *Journal of Sound and Vibration,* vol. 319, no. 1-2, pp. 91-118, 2009.

[7] P. Avitabile, Modal Testing: A Practitioner's Guide, Hoboken, NJ: The Society for Exper-

imental Mechanics and John Wiley & Sons Ltd, 2018.

[8] R. D. Blevins, Fourmulas for Natural Frequency and Mode Shape, New York: Van Nostrand Reinhold Co., 1979.

[9] Z. Lu, Z. Wang, S. Masri and X. Lu, "Particle impact dampers: past, present, and future," *Struct. Control Health Monit.* , vol. 25, no. 1, p. e2058, 2017.

[10] G. Michon, A. Almajid and G. Aridon, "Soft hollow particle damping identification in honeycomb structures," *J. Sound Vib.*, vol. 332, no. 3, pp. 536-544, 2013.

[11] Z. Xia, X. Liu, Y. Shan and X. Li, "Coupling simulation algorithm of discrete element method and finite element method for particle damper," *J. Low Freq. Noise Vib. Act. Control*, vol. 28, no. 3, pp. 197-204, 2009.

[12] Z. Xu, M. Wang and T. Chen, "Particle damping for passive vibration suppression: numerical modelling and experimental investigation," *J. Sound Vib.*, vol. 279, no. 3, pp. 1097-1120, 2005.

[13] Z. Lu, X. Lu, H. Jiang and S. Masri, "Discrete element method simulation and experimental validation of particle damper system," *Eng. Comput.* , vol. 31, no. 4, pp. 810-823, 2014.